Simulations of a Cold Front by Cloud-Resolving, Limited-Area, and Large-Scale Models, and a Model Evaluation Using In Situ and Satellite Observations

B. F. RYAN,* J. J. KATZFEY,* D. J. ABBS,* C. JAKOB,+ U. LOHMANN,# B. ROCKEL,@ L. D. ROTSTAYN,* R. E. STEWART,& K. K. SZETO,& G. TSELIOUDIS,** AND M. K. YAU++

* *CSIRO Atmospheric Research, Aspendale, Victoria, Australia*
+ *ECMWF, Reading, Berkshire, United Kingdom*
# *Department of Physics, Dalhousie University, Halifax, Nova Scotia, Canada*
@ *GKSS, Geesthacht, Germany*
& *Atmospheric Environment Service, Downsview, Ontario, Canada*
** *NASA Goddard Institute for Space Studies, New York, New York*
++ *Department of Atmospheric and Ocean Sciences, McGill University, Montreal, Quebec, Canada*

(Manuscript received 23 March 1999, in final form 3 January 2000)

ABSTRACT

The Global Energy and Water Cycle Experiment has identified the poor representation of clouds in atmospheric general circulation models as one of the major impediments for the use of these models in reliably predicting future climate change. One of the most commonly encountered types of cloud system in midlatitudes is that associated with cyclones. The purpose of this study is to investigate the representation of frontal cloud systems in a hierarchy of models in order to identify their relative weaknesses. The hierarchy of models was classified according to the horizontal resolution: cloud-resolving models (5-km resolution), limited-area models (20-km resolution), coarse-grid single-column models (300 km), and an atmospheric general circulation model (>100 km). The models were evaluated using both in situ and satellite data.

The study shows, as expected, that the higher-resolution models give a more complete description of the front and capture many of the observed nonlinear features of the front. At the low resolution, the simulations are unable to capture the front accurately due to the lack of the nonlinear features seen in the high-resolution simulations. The model intercomparison identified problems in applying single-column models to rapidly advecting baroclinic systems. Mesoscale circulations driven by subgrid-scale dynamical, thermodynamical, and microphysical processes are identified as an important feedback mechanism linking the frontal circulations and the cloud field. Finally it is shown that the same techniques used to validate climatological studies with International Satellite Cloud Climatology Project data are also valid for case studies, thereby providing a methodology to generalize the single case studies to climatological studies.

1. Introduction

The Global Energy and Water Cycle Experiment (GEWEX) has identified the poor representation of clouds in atmospheric general circulation models (AGCMs) as one of the major impediments for the use of these models in reliably predicting future climate change (see, e.g., Moncrieff and Tao 1999). The GEWEX Cloud System Study (GCSS) program was initiated in order to aid the improvement of cloud parameterizations (Browning et al. 1993). A major goal of GCSS is to make use of high-resolution cloud-resolving models in the development of layer and convective cloud representations for AGCMs.

One of the most commonly encountered types of cloud system in midlatitudes is that associated with cyclones. The complex dynamics driving these systems give rise to a variety of cloud types (Browning 1990; Lau and Crane 1995). This complexity, coupled with their common occurrence, makes extratropical layer cloud systems a natural candidate for GCSS activity on the representation of these cloud systems in AGCMs.

A natural first step to improve AGCM simulations of extratropical cloud systems is to establish the hierarchy of state-of-the-art models needed to achieve this goal. This study reports on the simulation of an extratropical cloud system observed during the Australian Cold Fronts Research Program (Ryan et al. 1989) using such a hierarchy of models. The purpose of this study is to investigate the representation of frontal cloud systems in a hierarchy of models in order to identify their relative weaknesses. The hierarchy of models was classified according to the horizontal resolution: cloud-resolving models (CRMs, 5-km resolution), limited-area models

Corresponding author address: Dr. Brian F. Ryan, CSIRO, Division of Atmospheric Research, Private Bag 1, 3195 Aspendale, Australia. E-mail: brian.ryan@dar.csiro.au

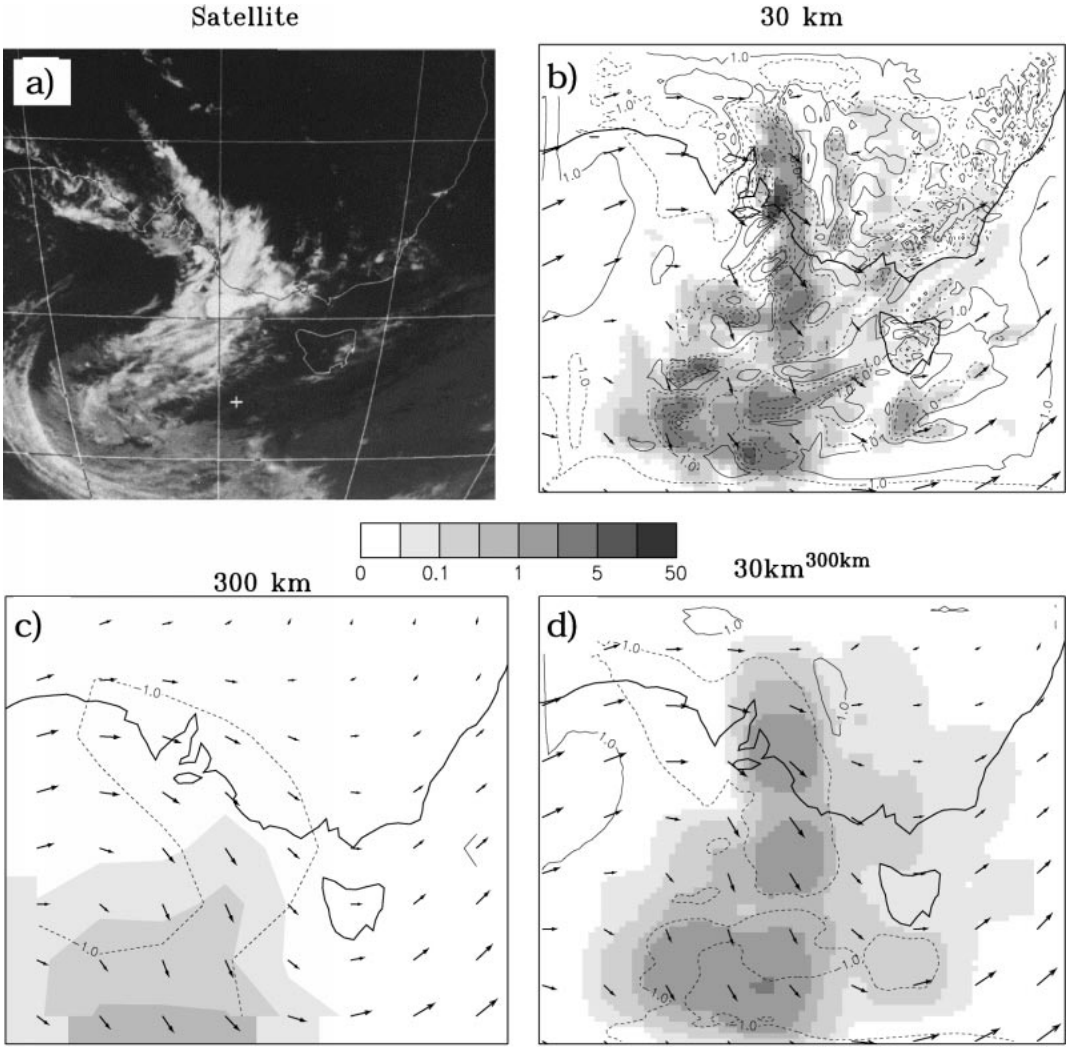

FIG. 1. (a) The GMS imagery at 0900 UTC 18 Nov 1984; (b) vertically integrated cloud and rainwater (shaded g kg^{-1}), vertical motion at 500 hPa (contours, Pa s^{-1}), and 500-hPa wind vectors from the CSIRO LAM (BFR) simulation at 30-km resolution at 0900 UTC 18 Nov 1984 (from Kazfey and Ryan (2000); (c) the simulation at 300-km resolution; and (d) the 30-km simulation averaged onto a 300-km grid.

(LAMs, 20-km resolution) and coarse-grid models (AGCMs and LAMs, >100 km).

In earlier studies, GCSS working groups have used single-column model (SCM) versions of AGCMs (Randall et al. 1996) to make the problem more tractable. It is not obvious that this technique can be applied in the highly advective and baroclinic situations usually encountered in frontal cloud systems. Two SCMs are used in this study to gain experience in the use of this model type for frontal cloud simulations. Apart from establishing the state of the art for cloud simulations using different model types, this study attempts to highlight deficiencies in the low-resolution models based on the high-resolution simulations. Since this is the first study of this kind, some of the results are preliminary.

The complexity of evaluating the physical representation of subgrid-scale cloud processes in an extratropical cloud system modeled by an AGCM is illustrated in Fig. 1. Figure 1a shows an observed cloud distribution for the case study used in this paper. Figure 1b shows the cloud distribution simulated by a typical state-of-the-art 30-km resolution mesoscale model with an explicit cloud scheme (Katzfey and Ryan 2000). Figure 1c shows the cloud distribution simulated by the same model but run at 300-km resolution (the typical grid resolution of climate models). Figure 1d shows the cloud distribution of the 30-km simulation when averaged to a 300-km grid (or what one might expect the 300-km simulation should capture). The spatial distribution of the vertically integrated cloud and rainwater from the 30-km simulation agrees reasonably well with the cloud cover in the Geostationary Meteorological Satellite (GMS) imagery. There is a lack of both vertical motion and vertically integrated liquid water in the 300-km run.

The 30-km-averaged simulation averaged onto the 300-km grid has stronger vertical motion and more vertically integrated cloud water than the 300-km simulation. Katzfey and Ryan (2000) showed that the lack of integrated cloud water in the 300-km resolution simulation was a result of weak vertical motions and was not due to a lack of moisture in the conveyor belt.

Both the AGCMs and the available analysis data used to provide initial and boundary conditions for the CRMs are extremely coarse and therefore a stepwise nesting technique needs to be applied in both initializing and running simulations using the CRMs. Hence there is a need to perform a set of intermediate simulations using LAMs with 20-km horizontal resolution. The 20-km simulations are typical of the resolution used by LAMs for regional numerical weather prediction. The LAM simulations provide the boundary conditions for the high-resolution CRM simulations. The most direct comparison to AGCMs can be achieved by using them to create a numerical forecast of the cloud system under study. A significant caveat of this approach is that most AGCMs developed for climate simulations are unable to run a numerical forecast for the system in question unless appropriate initial conditions are provided. In this study, the European Centre for Medium-Range Weather Forecasts (ECMWF) global forecast model was used to carry out the AGCM simulations.

One of the practical consequences of using a hierarchy of models to investigate the impact of subgrid-scale clouds on AGCMs was that each model used their own parameterizations. While all of the microphysical schemes in the LAMs, CRMs, and SCMs were bulk microphysical schemes, there were significant differences in the details of the formulation and assumptions used in the parameterizations. For example, the ice phase was carried as a single variable in some models and as five variables in other models.

A major problem in judging the performance of models is the availability of data for comparison. The two sources of data used in this study are the cloud information retrieved by the International Satellite Cloud Climatology Project (ISCCP; Rossow and Schiffer 1991) and the in situ data from the Cold Fronts Research Program (Ryan et al. 1985b). The ISCCP data have found wide application in climatological and AGCM evaluation studies. The novel approach taken in this paper is to use the ISCCP data in the evaluation of high-resolution cloud simulations.

After describing the details of the data (section 2) and the models used in this study (section 3), section 4 describes the main results of the model-to-data and model-to-model comparisons. Section 5 discusses the main findings with conclusions drawn in section 6.

2. Observations

In the warmer months from spring to autumn, surface troughs are a common feature of the low-level atmospheric circulation over Australia. Event 1 from Phase III of the Australian Cold Fronts Research Program (CFRP) was a ''typical'' summertime cool change that passed over southern Australia during the period 18–19 November 1984. Development occurred on the westerly prefrontal trough (Ryan et al. 1985b) and the observing network captured the evolution of the prefrontal subcloud layer on the subsynoptic (2000–200 km) and mesoscale (200–20 km). The observing network consisted of surface stations, rawinsondes, radars, and research aircraft (Ryan et al. 1989). There were two ships off the coast, one making hourly rawinsonde ascents and the other hourly radiosonde ascents (Fig. 2). In addition, a research aircraft flew missions to intersect the front with the flight plans focusing on the boundary layer.

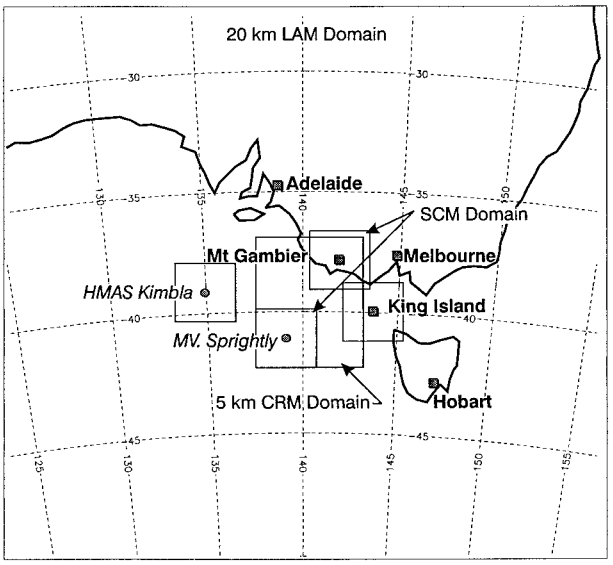

FIG. 2. The observational upper-air network for Phase 3 of the CFRP and the domains for the 20-km LAM, 5-km CRM, and the 300-km SCM simulations. The Bureau of Meteorology upper-air stations at Adelaide, Mount Gambier, Melbourne, and Hobart as well as the special CFRP upper-air stations King Island, the HMAS *Kimbla*, and the M/V *Sprightly* are shown.

a. ISCCP

Cloud properties were determined using data from ISCCP; (Rossow and Schiffer 1991), mainly consisting of cloud-top pressure and cloud optical thickness retrieved from satellite measurements of infrared and visible radiances. ISCCP analyses for this front diagnosed the cloud-top pressure of the prefrontal cloud between 300 and 400 hPa in the vicinity of the ships with some clouds up to 200 hPa (cloud-top pressure near the Mount Gambier land station). The ISCCP data are supported by the radiosonde ascents from the ships and the land station. The radiosonde ascents also suggest that cloud layering was sometimes present. In ISCCP terminology thin cloud has an optical thickness less than 10 and thick cloud has an optical thickness greater than 10. By this

definition cloud with an ice water content of less than 10^{-2} g kg^{-1} is classed as thin cloud if it occurred in a layer that was less than 100 hPa deep.

b. In situ data

Analysis of the subsynoptic rawinsonde network over the region showed that the cool change had the classical warm and cold conveyor belts (see, e.g., Browning 1990). The middle-level cloud ahead of the front was generated within the ascending warm conveyor belt. The absence of moisture sources in the continental boundary layer gave rise to high cloud bases (about 700 hPa) near 0°C ahead of the front. The warm conveyor belt generally occurred in a region of potential instability giving rise to embedded convection.

Station observations, and satellite and radar imagery showed that the rear edges of the cloud bands were well correlated with the surface pressure jumps and the radar echoes (see Fig. 12 in Ryan et al. 1989). The observed radar reflectivities correspond to rainfall rates ~2 mm h^{-1} and the precipitation bands were roughly parallel to the front with the spacing between bands of some 30–70 km.

The 24-h precipitation over the land in the model domain for the period from 0000 UTC on 18 November to 0000 UTC on 19 November shows that amounts of up to 10 mm occurred as the cloud system passed across southeastern Australia. Near the coast most of the rainfall was associated with convective rainbands with amounts ranging from 3 to 6 mm. There were no rainfall measurements over the ocean. However, an indication of the cloud and precipitation development can be gained from the oceanic surface observing stations, HMAS *Kimbla*, M/V *Sprightly*, and King Island. The hourly reports from these stations indicated that virga and intermittent rain were observed in the atmosphere preceding the surface cold front, consistent with the observations over the land.

The prefrontal air was warm and dry in the subcloud layer while the postfrontal air was cool and moist. There was strong ascent in the air ahead of the front while the heat and moisture budgets showed there was heating inside the cloud layer and cooling in the subcloud layer. Aircraft measurements confirmed that cloud base was 3–4 km, with bands of virga and showers reaching the ground. Evaporatively cooled downdrafts on a horizontal scale of 10–20 km were observed. Finally, a sharp wind shift and a sharp decrease in wet-bulb potential temperature were used to identify the arrival of the cold front.

Microphysical measurements were not made within this specific cloud system, although the microphysical characteristics of these systems have been documented (see King 1982; Ryan et al. 1985a). The prefrontal clouds associated with these systems rarely contain liquid water when the tops are colder than −12°C.

3. Model description

The CRMs were run at 5-km resolution in the horizontal and a stretched vertical grid with spacing that varied from 80 m at the lowest level to 1.5 km at the top. The LAMs were run at 20-km resolution in the horizontal and 18 levels in the vertical. Finally an AGCM weather prediction model was run at about 125-km resolution and compared with the 300-km LAM run by Katzfey and Ryan (2000). The SCM domain was a 300 km by 300 km box.

The LAMS were used to define the life cycle of the system and the synoptic and mesoscale forcing, thereby providing appropriate boundary conditions for the CRMs in this study. The boundary forcing for the SCMs was also derived from the LAMS. The locations of the single-column simulations are shown in Fig. 2.

a. Cloud-resolving models

The results from the cloud-resolving models have been examined in order to present the most detailed depiction of the development of the cloud system. The progressively coarser model results will then be examined and compared with the CRM results.

The cloud-resolving models used were the Canadian Mesoscale Compressible Community (MC2) (Benoit et al. 1997), the German GESIMA (Gesthachter Simulations Model der Atmosphäre) (Kapitza and Eppel 1992; Eppel et al. 1995), and Regional Atmospheric Modeling System (RAMS) (Tremback et al. 1986) run by CSIRO (Table 1). The CRM domain was a 600 km (N–S) by 500 km (E–W) box with the southwest corner 150 km south and 150 km west of the M/V *Sprightly* (Fig. 2). RAMS and MC2 were run with 25 vertical levels while GESIMA was run with 24 levels in the vertical. All the models had a vertical resolution of about 150 m in the boundary layer and about 800 m at 5 km.

Convective parameterizations were not used in the CRM simulations, and cloud processes were represented by bulk water microphysical schemes of various complexities. The Kong–Yau bulk water cloud scheme (Kong and Yau 1997) used in the MC2 simulation included five water species, namely vapor, cloud water, cloud ice/snow, graupel, and rain. The bulk microphysical parameterization scheme used by RAMS (Flatau et al. 1989) predicts the total water mixing ratio and the mixing ratios of rain droplets, pristine ice crystals, snow, aggregates, and graupel particles. The mixing ratios of water vapor and cloud droplets are diagnosed. Ice crystal nucleation includes heterogeneous and homogeneous nucleation and the generation of ice crystals by riming. The cloud scheme in GESIMA is described by Levkov et al. (1992). The parameterized microphysical processes in all the schemes typically include condensation/evaporation, autoconversion, accretion, heterogeneous and homogeneous nucleation of ice nu-

TABLE 1. Model characteristics.

Model	Resolution	Non-hydrostatic	Microphysics	Convection
ECMWF	T106	No	Tiedke (1993)	Tiedke (1989)
DARLAM (BFR)	20 km	No	Katzfey and Ryan (1997)	McGregor et al. (1993)
DARLAM (LDR)	30 km	No	Rotstayn (1977)	McGregor et al. (1993)
MC2	20 km	Yes	Kong and Yau (1997)	Kuo (1974)
REMO	20 km	No	Levkov et al. (1992)	Tiedtke (1989)
RAMS	20 km	Yes	Flatau et al. (1992)	Chen and Frank (1993)
RAMS	20 km	Yes	Flatau et al. (1992)	Kuo (1974)
MC2	5 km	Yes	Kong and Yau (1997)	None
GESIMA	5 km	Yes	Levkov et al. (1992)	None
RAMS	5 km	Yes	Flatau et al. (1992)	None
CCCma	300 km	No	Lohmann et al. (1999)	Zhang and McFarlane (1995)
ECHAM	300 km	No	Lohmann and Roeckner (1995)	Tiedtke (1989)

clei, deposition/sublimation, freezing/melting, and riming.

The choice of horizontal resolution for the CRMs represented a compromise between available computing power and an optimal representation of the frontal situations. No cumulus parameterization was used in the simulations since there is no suitable cumulus scheme available for use with the chosen model resolution. In addition, the frontal precipitation was very weak with radar reflectivities of 28 dBZ (corresponding to a rainfall rate $\sim$2 mm h^{-1}) or less. These radar signatures were associated with the convective bands, although some isolated showers containing small areas of more intense rainfall were reported. It was therefore decided that the CRM resolution was able to capture the passage of the front and the associated cloud motions. The cirrus circulations were not considered to be important at the time of designing the experiment, although this is probably an incorrect assumption, as will be shown later.

b. Limited-area models

The LAMs used at 20-km resolution were (i) DARLAM (BFR, Katzfey and Ryan, 1997) run by CSIRO, Australia; (ii) RAMS (Tremback et al. 1986) run by CSIRO, Australia; (iii) MC2 run by the Atmospheric Environment Service, Canada (Benoit et al. 1997); and (iv) REMO run by GKSS, Germany (Majewski 1991; Karstens et al. 1996). In addition DARLAM (LDR; Rotstayn 1997) was rerun at 30-km resolution using the cloud scheme developed for the CSIRO AGCM. Table 1 summarizes the characteristics of the LAMs.

The initial and boundary conditions for the limited area simulations were obtained from the 6-hourly reanalyzed ECMWF fields (Gibson et al. 1997) interpolated to a 20-km grid. The location of the southwest corner of the domain was 50°S, 120°E and the location of the northeast corner of the domain was 20°S, 155°E. The validating fields were the same as those analyzed for the CRM simulations.

c. Coarse-grid and single-column models

The numerical weather prediction model was the ECMWF global model run at spectral resolution T106 corresponding to a grid of 125 km using 31 model levels in the vertical. The SCM models used were the Canadian SCM (CCCma) and the German SCM (ECHAM). The two SCMs used the same vertical resolution as DARLAM and had the same time step of 20 min. The cloud physics scheme used in the ECHAM-SCM is described in Lohmann and Roeckner (1995) while the scheme used in CCCma is described in Lohmann et al. (1999). Both SCMs employ prognostic equations for cloud water and cloud ice. In ECHAM, the Sundqvist et al. (1989) parameterization for cloud cover was used, while a statistical approach was used in CCCma.

The SCM experiment was designed such that it (i) used only the ocean as the lower boundary and (ii) was forced by the advection and vertical velocity recomputed from 300-km box-averaged variables from DARLAM. This treatment of the advection was aimed to mimic more closely that used in the AGCM. The temperature and surface pressure were provided as lower boundary conditions. The forcing (horizontal plus vertical advection of temperature, specific humidity, and cloud water) and the vertical velocity to calculate the adiabatic compression/expansion were provided from DARLAM.

4. Results

a. CRMs versus data

The CRM simulations generated a frontal system with considerable structure. An important question to be answered is whether the finescale structure was also observed in the real system and, in particular, whether the 5-km simulation captured the essential motions associated with the passage of the cool change. Figure 3 shows the vertical velocities at 600 hPa and the surface precipitation rates from the MC2 CRM results at 0800 UTC 18 November. Several bands of strong vertical

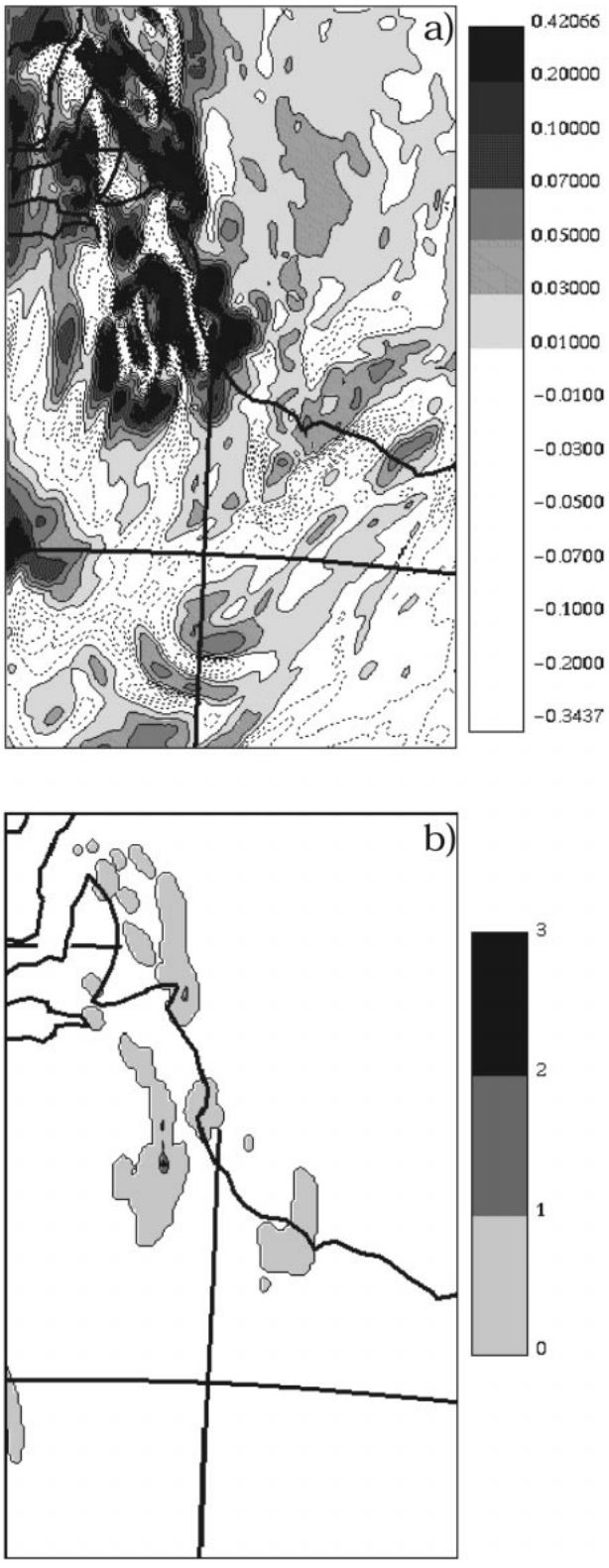

FIG. 3. (a) Vertical velocities (m s^{-1}) at 600 hPa and (b) surface precipitation rates (mm h^{-1}) from the MC2 CRM simulation valid at 0800 UTC 18 Nov.

ascent are evident in the CRM results (Fig. 3a), giving rise to cloud bands (not shown). Satellite and radar pictures of the system taken at about the same time (see Fig. 12 of Ryan et al. 1989) indicated four cloud bands ahead of the system: three weaker bands located far ahead of the front, and one strong band located near the front. The horizontal separations of the observed cloud bands were quite similar to the ones in the model results. However, the observed bands were mainly over the ocean, whereas the simulated bands were closer to the coastline. Only two of the simulated cloud bands produced precipitation at the surface (Fig. 3b). When compared with the radar images of the case near the same time (Fig. 12b of Ryan et al. 1989), the locations of the two simulated rainbands agree extremely well with the observed ones. The 5-km simulation captured the rainbands but would not have resolved the observed individual updrafts and downdrafts that were on the horizontal scale of 10 km. There are no observations to determine the vertical and horizontal scales of the upper level cirrus. However, during Phase II of the First ISCCP Regional Experiment (FIRE II), Gultepe et al. (1995) found that coherent structures formed in cirrus generated in upper-tropospheric flows had horizontal scales of between 0.2 and 10 km. The CRM simulation did not have the horizontal resolution to resolve motions in this scale range.

b. CRMs intercomparison

There are similarities and differences within the CRM simulations. In general, the frontal thermal contrast and overall frontal cloud features are similar but there are significant differences between the models in the fine-scale cloud characteristics. The cold front in all three models crossed Mount Gambier at approximately 1500 UTC 18 November. Similar prefrontal mesohighs, as discussed in Ryan et al. (1989), were also observed in all three simulations. The accumulated precipitation at Mount Gambier is about 6 mm in MC2 and about 2–3 mm in the RAMS run. These accumulated precipitation amounts are within the observed range of 3–6-mm accumulation in the coastal region. Slightly less precipitation (approximately 1.5 mm) was obtained in the GESIM simulation.

The time–pressure cross sections of the box-average total cloud water and ice (pristine and precipitating) mixing ratios and vertical velocity over M/V *Sprightly* from the MC2, RAMS, and GESIMA runs are given in Fig. 4. All three CRMs captured the development of the prefrontal cloud. However, there is less high cloud and more middle-level cloud in the GESIMA and RAMS simulations (Figs. 4b,c). The prefrontal middle-level cloud cover and the temporal extent (between approximately 0700 and 1700 UTC) of the frontal cloud cover are comparable in all the model results. In each case, the middle-level cloud was mostly ice and extended from approximately 700 to 400 hPa, which is in agree-

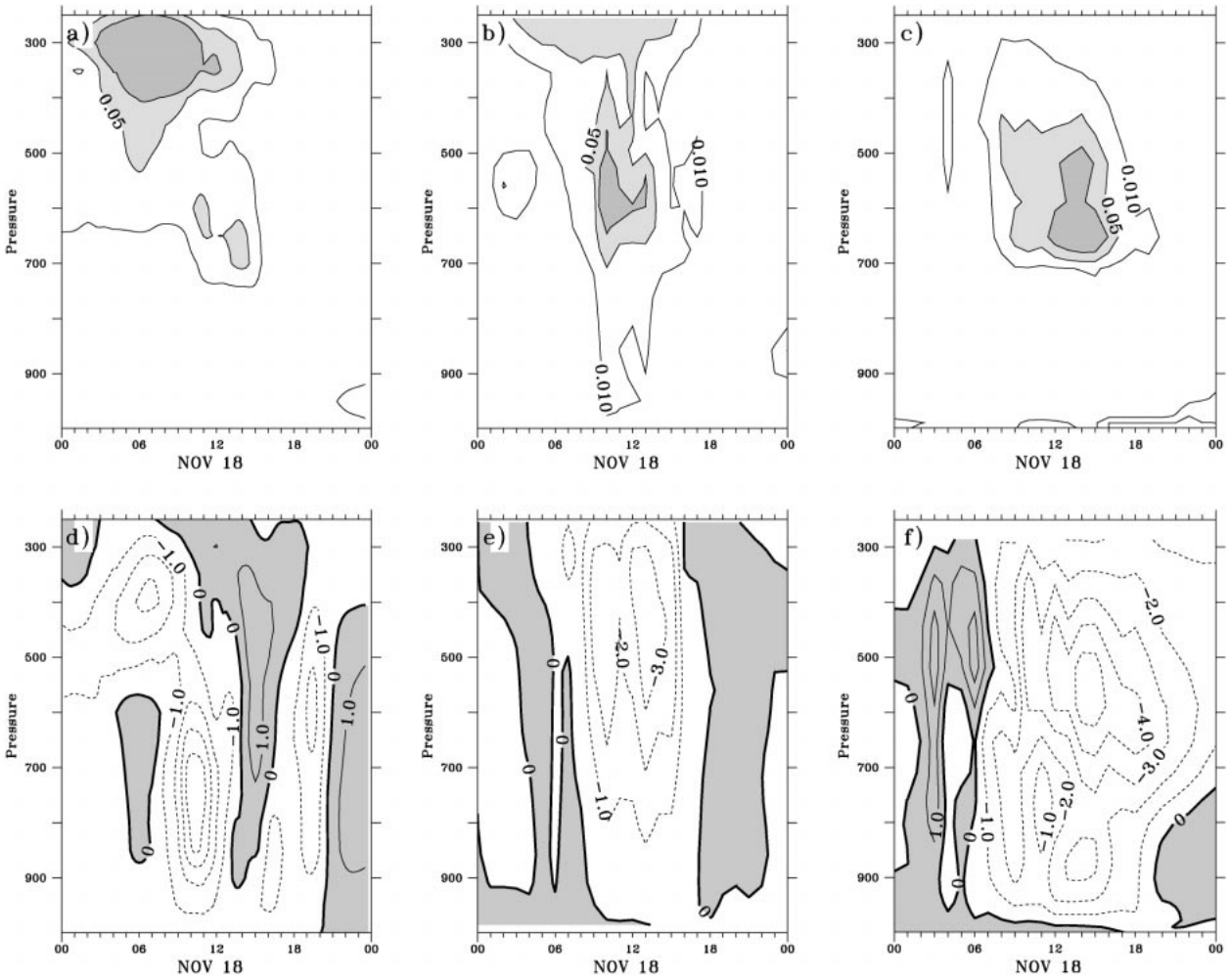

FIG. 4. The time–pressure cross sections for the 300 km × 300 km box over the M/V *Sprightly* of average ice and cloud water mixing ratios (g kg^{-1}) from (a) MC2, (b) GESIMA, and (c) RAMS. The minimum contour is 0.01 g kg^{-1} and vertical velocities (Pa s^{-1}): (d) MC2, (e) GESIMA, and (f) RAMS.

ment with the observations of Ryan et al. (1985a). The mean frontal updraft has similar magnitude among the cases. In the MC2 simulation, the upper-level clouds at 0600 18 November generated evaporative cooling (Fig. 5c) and subsidence below cloud base (Fig. 5a). This weak subsidence below 700 hPa was absent in the GESIMA and RAMS results.

c. LAMs versus data

The CRMs were able to capture much of the finescale detail of the clouds and rainbands. The coarser 20-km LAM simulations are now examined to see how effectively they captured the frontal cloud.

ISCCP data have been widely used in climatological application to evaluate studies using AGCMs. The same techniques can also be applied on much smaller spatial scales to evaluate the studies using the LAMs. Figure 6 shows the cloud-top pressure (top panel) and cloud optical thickness (middle panel) from ISCCP data (left) and the 20-km DARLAM simulation (middle) as well as the difference between the two for 0000 UTC on 18 November (right). The lower panels of Fig. 6 show optical thickness–cloud-top pressure (TAU–CTP) histograms over the domain for the satellite retrievals and the model. Radiometric ISCCP definitions of cloud type are superimposed. This time period in the history of the system corresponds with the development phase, when the in situ field observations suggested that the prefrontal part of the cloud system consisted of layers of cirrus and middle-level altostratus and altocumulus. The satellite retrievals show similar cloud types, with the peaks of the cloud-type distribution in the altostratus, altocumulus, and cirrus categories. They also show a layer of low stratus and stratocumulus clouds upstream from the front. The DARLAM model captures correctly the broken nature of the cloud field and produces smaller low cloud amounts, particularly behind the front. Ahead

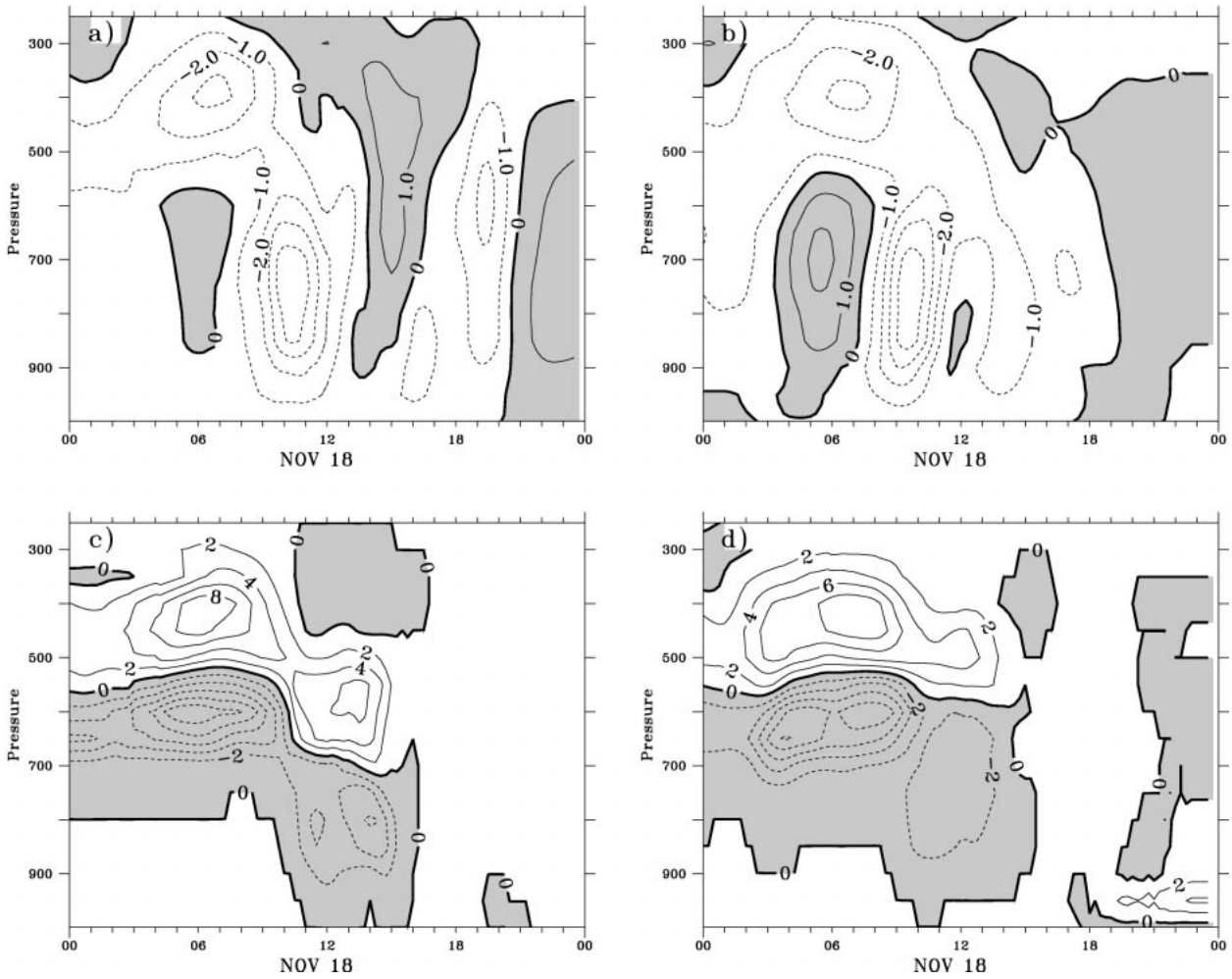

FIG. 5. Time–pressure cross sections for 300 km × 300 km mean variables centered over the M/V *Sprightly* for the MC2 CRM and LAM simulations: (a) omega (Pa s^{-1}) for MC2 CRM, (b) omega (Pa s^{-1}) for MC2 LAM, (c) total latent heating (K day^{-1}) for the MC2 CRM, and (d) total latent heating (K day^{-1}) for the MC2 LAM.

of the front, the model produces an extensive deck of high-level cloud, whereas the satellite retrievals show predominantly altocumulus cloud and altostratus cloud with smaller amounts of cirrus cloud. Along the frontal boundary the model simulates the layer of deep cloud classified as convective by the ISCCP analysis.

Figure 7 shows the same panels at 0000 UTC on 19 November and depicts the mature phase of the cloud system. The model accurately captures the main features of the frontal structure with both the model and the satellite retrievals showing the main peaks in cloud-type distribution in the stratocumulus, cirrus, and deep convection categories. However, there are still differences in the height of the prefrontal cirrus and the thickness of the postfrontal low clouds. The main differences are found in the tail of the front where the satellite retrievals show a layer of cirrus cloud, while the model produces deep frontal cloud and a clear air transition to the postfrontal low cloud deck. However, the most striking feature of the lower panels in Figs. 6 and 7 is the apparent absence of thin middle-level cloud diagnosed by the model.

A comparison of the synoptic fields of mean sea level pressure, moisture, and winds from the LAMs (not shown) indicates that all simulations captured this event reasonably accurately. However, most models moved the cold front too rapidly, possibly associated with a lack of evaporating precipitation (see Katzfey and Ryan 1997). The Mount Gambier station observations show that several mesohighs passed over the station, each associated with the passage of a rainband. However, in contrast to the CRMs, all of the LAM simulations produced a single rainband and the model station pressures at Mount Gambier and the M/V *Sprightly* showed a single pressure rise that coincided with the passage of a rainband.

At 20-km resolution the models gave rainfall totals comparable with the 4 mm observed at Mount Gambier. The most significant feature in the LAM simulations is that almost all the rain over Mount Gambier was gen-

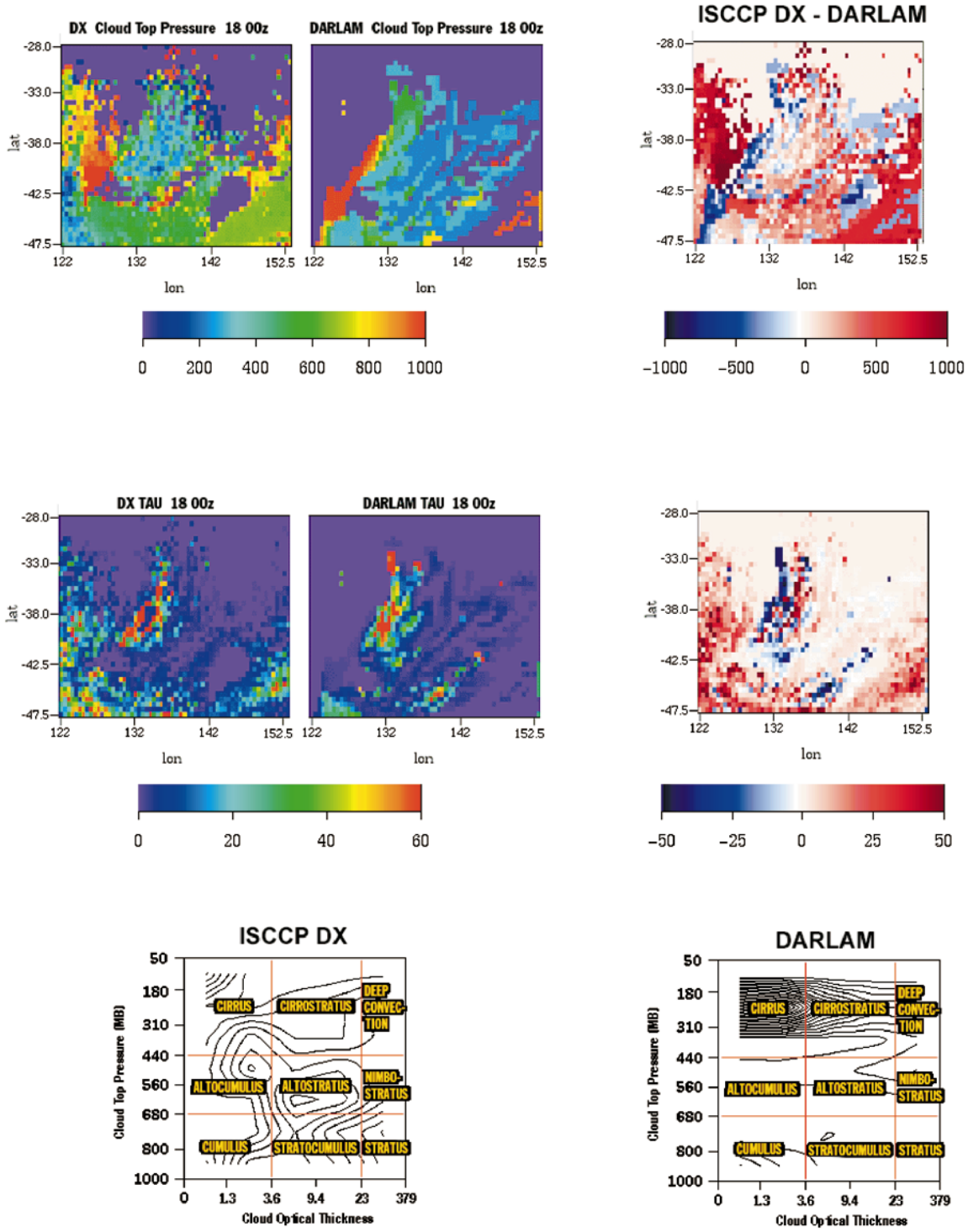

FIG. 6. (a) Cloud pressure (top) for ISCCP DX, DARLAM, and ISCCP DX − DARLAM at 0000 UTC 18 Nov 1984, (b) optical depth (middle) for ISCCP DX, DARLAM, and ISCCP DX − DARLAM at 0000 UTC 18 Nov 1984, and (c) the cloud-top pressure − optical depth histograms (bottom).

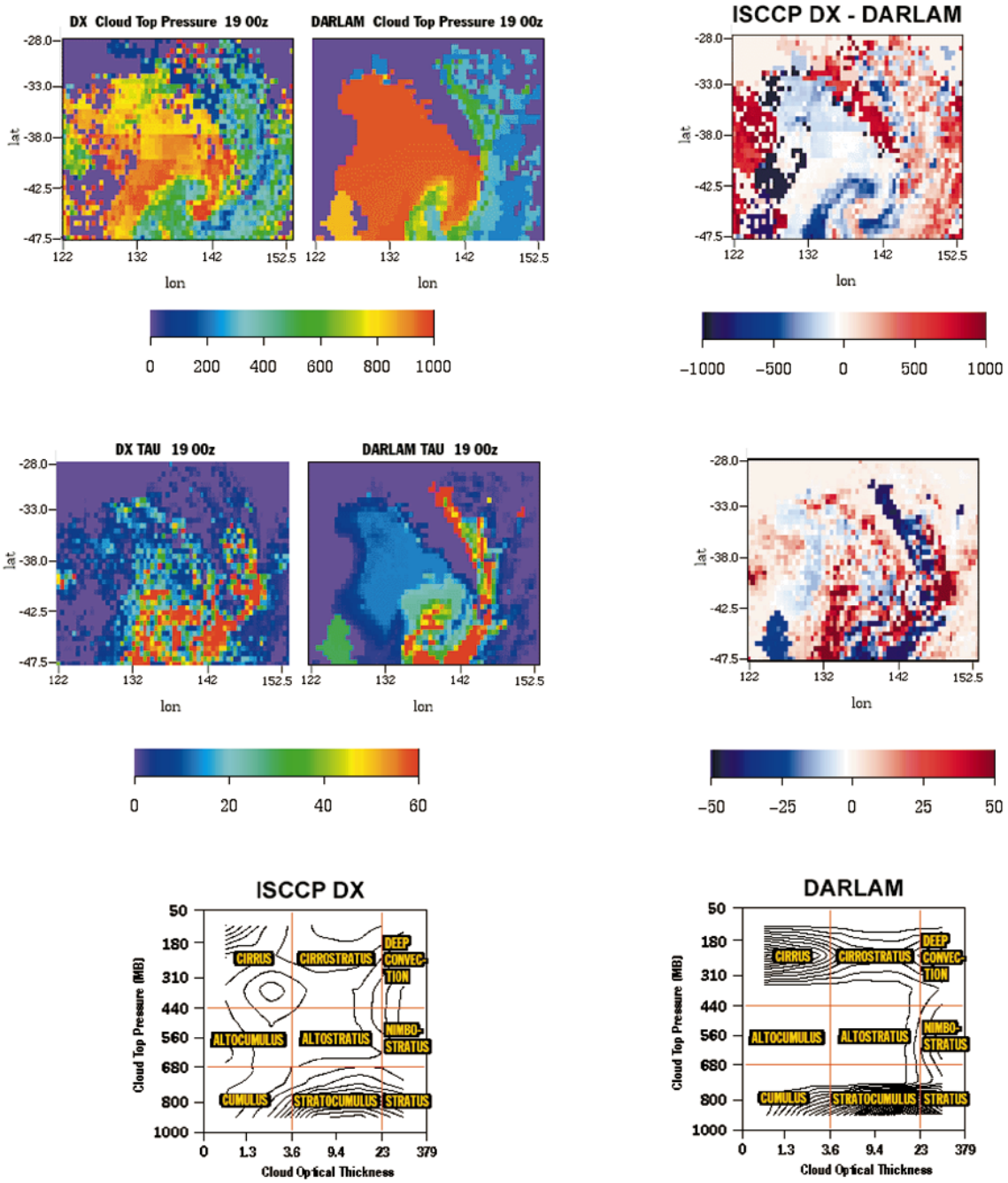

FIG. 7. (a) Cloud pressure (top) for ISCCP DX, DARLAM, and ISCCP DX − DARLAM at 0000 UTC 19 Nov 1984, (b) optical depth (middle) for ISCCP DX, DARLAM, and ISCCP DX − DARLAM at 0000 UTC 19 Nov 1984, and (c) the cloud-top pressure − optical depth histograms (bottom).

erated by the convective parameterizations and almost no rain was generated by the explicit cloud scheme. The exception was the RAMS simulation using the Frank–Chen–Cohen convective parameterization, which produced no convective rain over Mount Gambier; that is, all the rain was produced by the explicit microphysics. However, when the Frank–Chen–Cohen convective scheme (Frank and Cohen 1985, 1987; Chen and Frank 1993) in RAMS was replaced by the Kuo convective scheme, more convective rain was generated and the total rainfall was comparable to that produced with MC2, which also used the Kuo convection scheme. By contrast, it was the explicit cloud schemes that generated all the rainfall over the M/V *Sprightly* point for all LAM models.

The frontal transition zone passed over the M/V

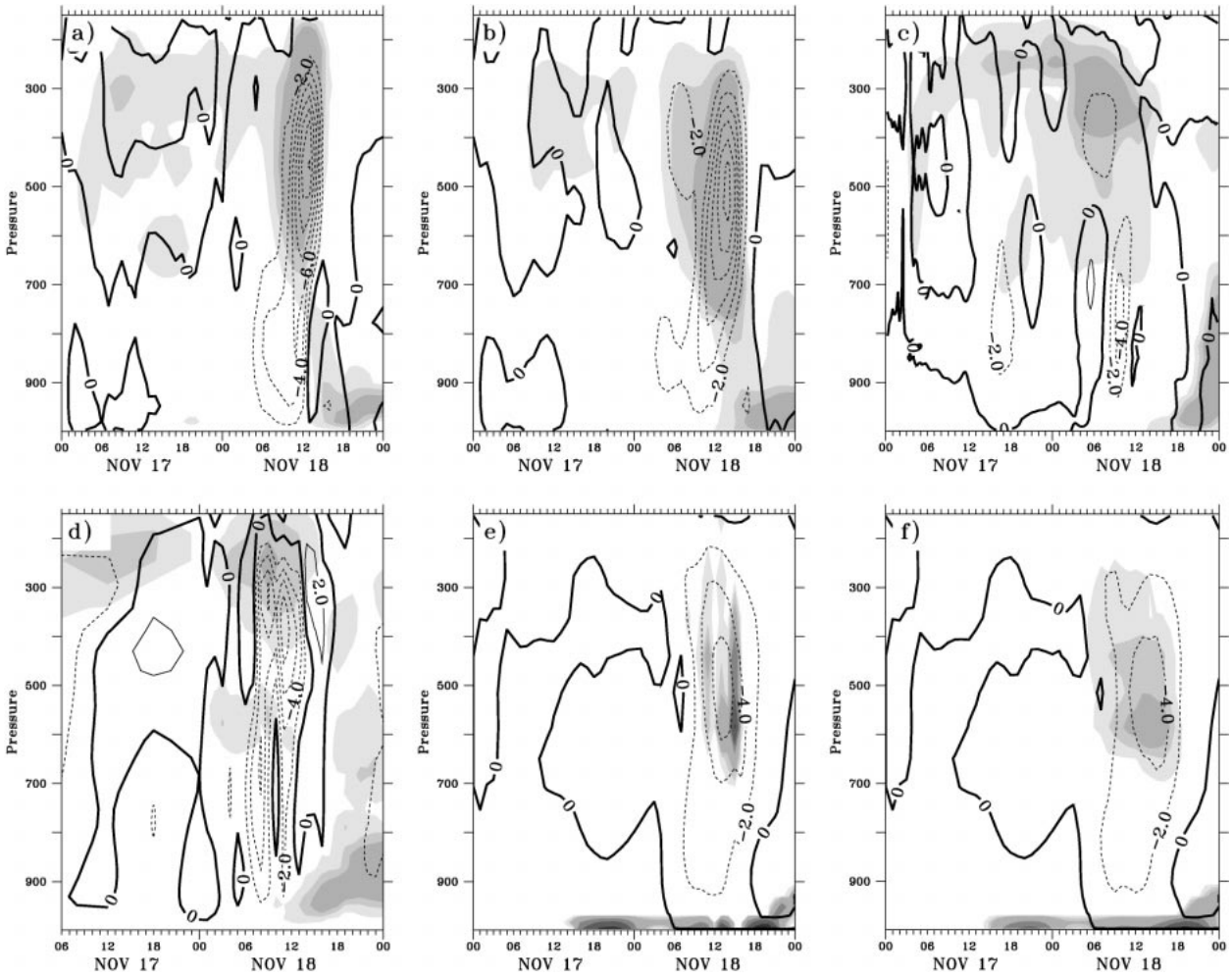

FIG. 8. The box-averaged omega (Pa s^{-1}) for the box centered on the M/V *Sprightly*: (a) DARLAM (BFR), (b) DARLAM (LDR), (c) MC2, (d) REMO, (e) RAMS (Frank–Chen–Cohen), and (f) RAMS (Kuo). The shaded region shows the box-averaged ice and cloud water mixing ratios. The lightest shading is 0.01 g kg^{-1}.

Sprightly between 0600 and 1600 UTC. All but the RAMS simulations form a cirrus layer about 12–24 h ahead of the front. This layer has a cloud top near 200 hPa and the layer is 100–200 hPa thick. The gridpoint ice and water contents (not shown) generate a broken prefrontal cloud-layer structure that is consistent with the cloud cover observations. The surface observations from M/V *Sprightly* show that upper-level clouds were observed at least 10 h ahead of the front. The soundings from the M/V *Sprightly* and Mount Gambier show signatures in the temperature and moisture fields that support the surface observations of virga falling from an altocumulus layer, and indicate that there were thin layers in the midtroposphere that could not be simulated by the LAMs. Figure 8 shows that the effect of averaging the cloud ice/water and vertical velocity fields over the 300-km box is to smooth all the fields. However, even when averaged it is quite clear from Fig. 8 that the vertical motions strongly control the presence of cloud. Figure 8 shows that all of the limited-area models fail to generate any significant prefrontal middle-level vertical motion and hence middle-level prefrontal cloud.

d. CRMs versus LAMs

More detailed and realistic frontal structures are evident in the CRM results. While the LAMS were unable to capture the multiple-rainband structure evident in the CRMs, some of them were able to capture the mesohigh associated with the rainfall near the front. The CRM results reproduced a little more prefrontal middle-level cloud than the LAMs but the use of higher model resolution did not eliminate the problem. Examination of the model results shows that the deficiency of prefrontal middle-level clouds might be related to the overprediction of prefrontal cirrus and the poorly handled subcloud sublimational cooling in the model frontal systems. The 5-km horizontal resolution is too coarse to accurately reproduce the narrow convective bands.

Some localized downdrafts were observed to occur on length scales ~10 km, and therefore further sensitivity experiments are needed to achieve the optimal model resolutions needed for this kind of system. Observation of cirrus generated by synoptic systems during FIRE II suggest that if the simulations are to reproduce the cirrus circulations, they would need to be modeled at a horizontal resolution of 1 km.

The impact of using higher model resolutions is evident in the box-averaged results. The time–pressure cross sections of 300 × 300 km box-averaged results centered over the *Sprightly* for the MC2 CRM and LAM runs are given in Fig. 5. The differences between the CRM and LAM results are more amplified in the Mount Gambier box (not shown). When the mean cloud fields from the two simulations were compared, there were more mesoscale structures in the CRM run. When compared to the observed Q1 budgets near Mount Gambier (see Fig. 11 of Ryan et al. 1989), the CRM reproduced both the magnitudes and the temporal evolution of the cloud latent heating and the subcloud evaporative cooling (Fig. 5c). It is also of interest to note that the stronger subcloud evaporative cooling in the CRM run produced mean subsidence below cloud base near Mount Gambier (not shown). These mean downdrafts were not evident in the LAM results.

There were more middle- and high-level clouds in the CRM simulation. The prefrontal middle-level cloud was not well captured in most of the LAM runs. In the M/V *Sprightly* box, the middle-level cloud amount from the MC2 CRM was only a slight improvement on the LAM simulation (Figs. 4a and 8c). However, the MC2 CRM generated considerably more cloud than the LAM simulation over the Mount Gambier box (not shown). The TAU–CTP histograms for the MC2 CRM results (not shown) also show this improvement over the LAM results when compared to the ISCCP results. However, a deficiency still exists in the amount of prefrontal middle-level cloud in the CRM run when compared to observations, especially over the M/V *Sprightly* region. An examination of the box-mean vertical velocities and heating budgets over the region shows a plausible explanation for this deficiency of the models. The prefrontal middle-level cloud was formed mainly by the deep, but weak, ascent of the warm air in the warm conveyor belt (see, e.g., the weak deep mean ascending motion in Figs. 5a and 5b between 0000 and 0300 UTC). There was also a thick prefrontal anvil formed above 400 hPa in about the same location (Figs. 4a and 8c). The ice particles that fell from the thick cirrus cloud deck produced substantial sublimational cooling below cloud base (see Figs. 5c and 5d between 700 and 520 hPa). This cooling induced a weak downdraft (see Figs. 5a and 5b between approximately 0400 and 0800 UTC), which inhibited the further development of the middle-level cloud layer until the stronger prefrontal rainband approached the region. While prefrontal cirrus cloud was observed in the real case, it appears to be overpredicted in all the models. In addition, since the sublimation of ice crystals occurs rapidly within a thin layer (Clough and Frank 1991), the relatively coarse vertical resolution used by the models at the upper troposphere might not resolve the associated cooling effect adequately.

These model results demonstrate the complicated coupling of different cloud components in frontal layer cloud systems as discussed in the introduction. For example, if convection is not handled well in the models, the cirrus deck formed by the detrainment from convective clouds will also be poorly predicted. This, in turn, can affect the development of prefrontal middle-level cloud, and so on. Each individual cloud component and their interactions must therefore be handled accurately in the models before the observed development of large-scale cloud fields can be reproduced in the models.

e. LAMs versus large-scale models and SCMs

1) LARGE-SCALE MODELS

As outlined in the introduction, one technique of simulating the CFRP frontal cloud system with an AGCM is through the use of a global numerical weather prediction model. This section illustrates the possible use of this method using a simulation of the system performed with the ECMWF global forecast model. The simulation was performed at T106 (about 125 km) resolution, which is close to the resolution of AGCMs currently used in climate studies. The advantage of using the full AGCM in ''weather forecast mode'' is that the cloud system is simulated in the ''proper'' model environment so that the difficulties of prescribing the forcing terms necessary in SCM simulations do not exist. The disadvantages are that initial conditions of high enough quality for a successful forecast need to be created. Here, the initial conditions are taken from the ECMWF reanalysis and are therefore the most suitable for the simulation. Errors in the large-scale model are normally small in the early stages of a simulation and therefore short-range forecasts (12–48 h) are used in the comparison.

The T106 simulation is compared to the DARLAM 30-km simulation and, the ''averaged'' DARLAM 30-km simulation, as well as the 300-km resolution DARLAM simulation from Katzfey and Ryan (2000). Figure 9 shows a snapshot of cloud and rainwater content for these simulations 36 h into the forecast. It is obvious that the low-resolution models (DARLAM 300, Fig. 9c and ECMWF T106, Fig. 9d) are not able to resolve any of the small-scale structure that is generated by the 30-km resolution DARLAM simulation. In fact the 300-km DARLAM simulation fails to predict even the large-scale structure of the cloud band. However, more interestingly, although the cloud structure is qualitatively similar in the ECMWF simulation to the averaged 30-

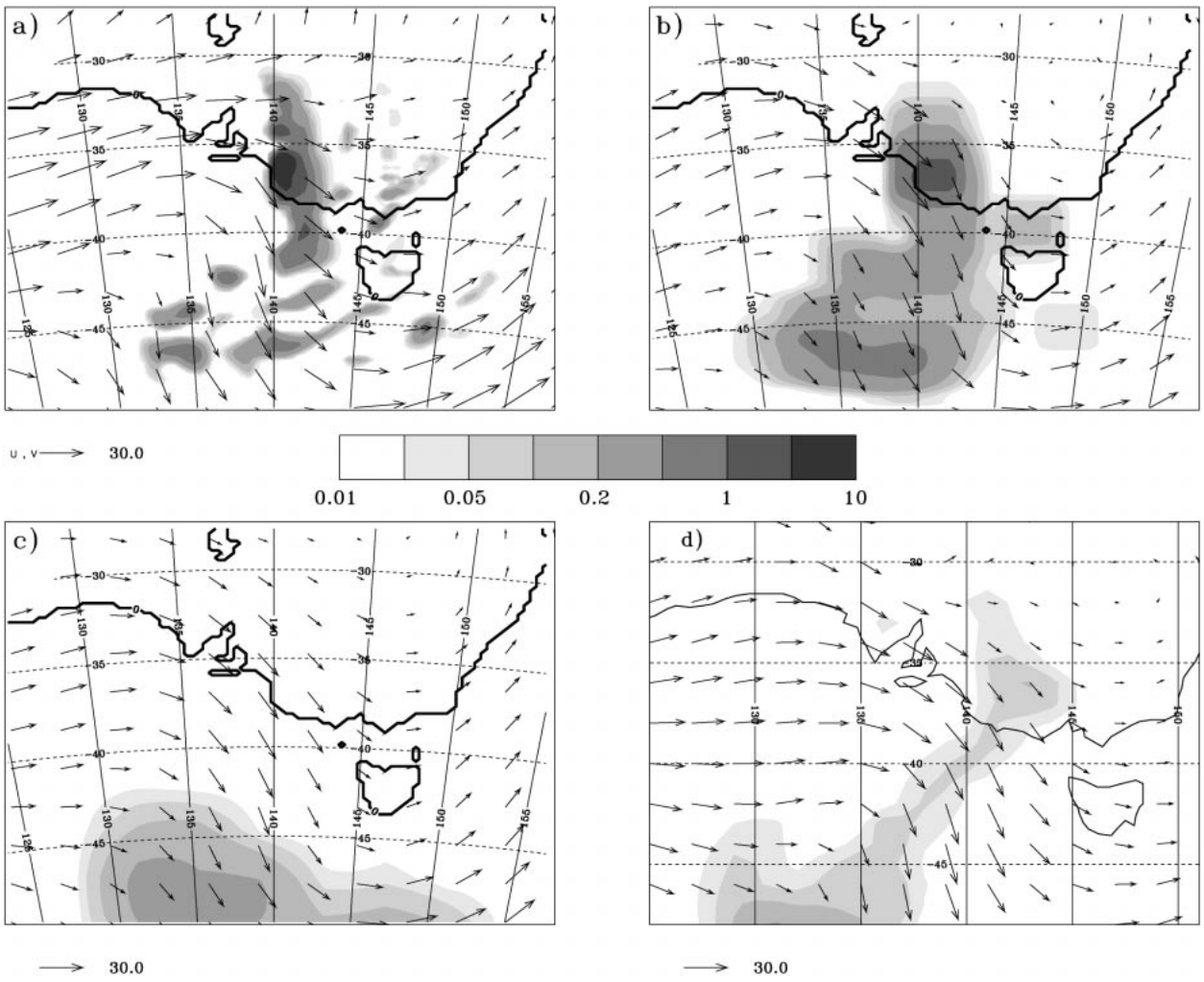

FIG. 9. Cloud and rain field (g kg^{-1}) and wind field at 600 hPa (arrows) for (a) the 30-km DARLAM simulation, (b) the 30-km DARLAM simulation averaged to 300 km and interpolated back to 30 km, (c) the 300-km DARLAM simulation interpolated to a 30-km grid, and (d) the ECMWF T106 simulation.

km simulation (Fig. 9b), the cloud water content is significantly lower. This might point to a parameterization deficiency in the AGCM. A possible reason could be that the use of large-scale vertical velocity to predict cloud in the front [see Tiedtke (1993) for a detailed description of the cloud parameterization] is insufficient, in which case some information on the subgrid vertical velocity distribution needs to be included. Imagine a grid box with sides of 300 km, in which vertical motion is arranged such that half the grid box experiences strong upward motion while the other half experiences strong downward motion. The ''large scale'' vertical motion in this case is zero; therefore, no condensation due to vertical motion can occur. However, a model resolving the mesoscale vertical motion would produce condensation, and hence cloud in half of the grid box, so that the average cloud water content would be nonzero. The comparison of the two models would hence be similar to that between the averaged DARLAM simulation and the ECMWF model shown here.

Figure 10 shows the gridpoint averages for cloud water/ice mixing ratios at the grid point closest to the M/V *Sprightly*. The grid points emphasize the smearing effect of the larger grid size. However, perhaps more significantly, the averaging of the LAM results onto the 300-km grid (Fig. 10b) gives the impression that the model generates a broad band of middle-level cloud, whereas in reality it is a thin band (Fig. 10a) that has been smeared by the averaging process. The ECMWF T106 also generates the middle-level cloud but fails to form any cirrus with ice mixing ratios exceeding 0.01 kg kg^{-1}, while there is virtually no frontal cloud in the 300-km LAM simulation.

The examples shown above do not provide a complete comparison of the AGCM results to the LAM simulations. However, they demonstrate the potential of this

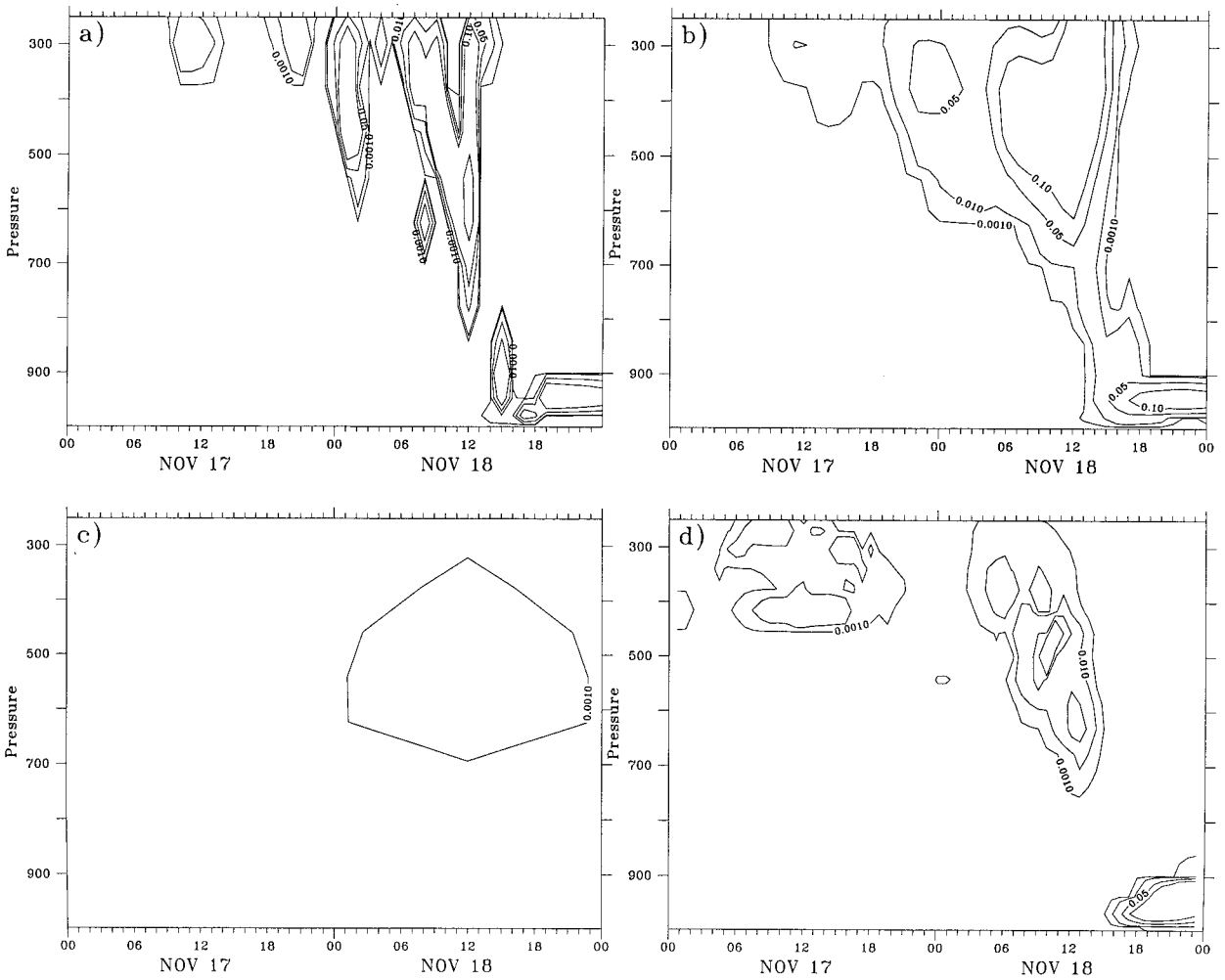

FIG. 10. Cloud and rain (g kg^{-1}) field over the grid point closest to the M/V *Sprightly* for the 30-km DARLAM simulation, (b) the 30-km DARLAM simulation averaged to 300 km and interpolated back to 30 km, (c) the 300-km DARLAM simulation interpolated to a 30-km grid, and (d) the ECMWF T106 simulation. The minimum contour is 0.01 g kg^{-1}.

method. A numerical weather prediction model provided with a reasonable initial state is a very powerful tool for these types of studies. AGCM simulations at a range of resolutions could be used to investigate the importance of existing and future parameterization assumptions for the simulation of the key features of a frontal cloud system as identified by the very high resolution simulations using LAMs and CRMs. Only a few AGCM groups at presently have access to this method. It is therefore necessary to investigate whether other (''cheaper'') methods are suitable for extratropical cloud systems such as SCMs.

2) SINGLE-COLUMN MODELS

Time sections of cloud water and ice for the M/V *Sprightly* column from the SCMs are shown in Figs. 11b and 11c. For comparison, cloud water and ice are also shown in Fig. 11a for DARLAM that was used to drive the SCMs. All experiments predict a thick altocumulus/altostratus layer at 0600 UTC on 17 November, which becomes thinner over the course of the day. Maximum cloud water in DARLAM and CCCma is simulated prior to the frontal passage at 1400 UTC on 18 November in the midtroposphere. Only in DARLAM does the cloud extend vertically from the surface up to 200 hPa after the prefrontal cloud band has passed. In the SCMs, the clouds do not reach the surface. CCCma simulates no postfrontal cloud at all, while ECHAM simulates stratiform clouds of large vertical extent and high ice content. The overestimation of these clouds in ECHAM may be caused by ECHAM having a lower threshold in relative humidity for the onset of cloud formation than DARLAM. Condensation in ECHAM starts at relative humidities below 100% if adiabatic cooling and/or moisture advection occur. Both processes act after 1800 UTC on 18 November as well as at the

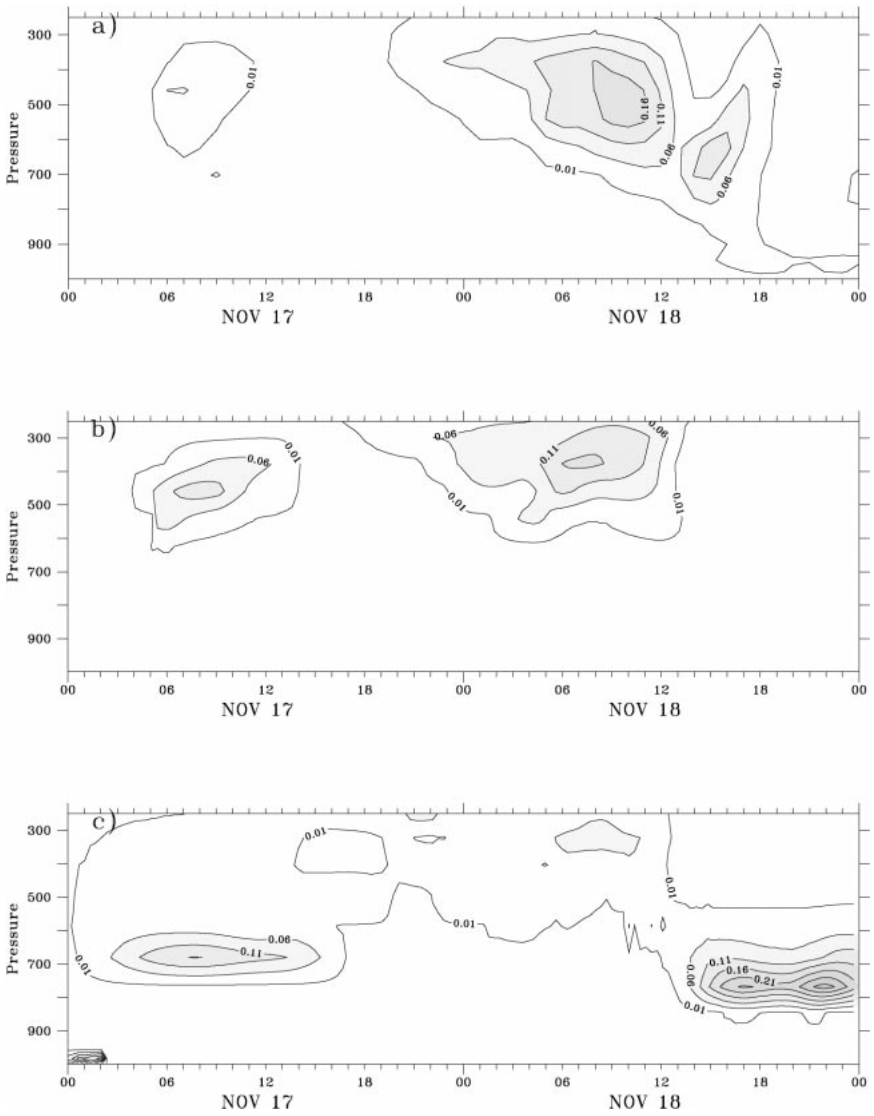

FIG. 11. Cloud water (g kg^{-1}) for the M/V *Sprightly* column (a) DARLAM (BFR), (b) CCCma and (c) ECHAM. The minimum contour is 0.01 g kg^{-1}.

beginning of the simulation where only ECHAM creates clouds at 700 hPa.

The time series of vertically integrated cloud water path (sum of cloud liquid water and ice), cloud cover, and precipitation for the M/V *Sprightly* regions are shown in Fig. 12. Total cloud cover is also extracted from the observers' reports. In the M/V *Sprightly* grid box, ECHAM (dashed line) and CCCma (solid line) suggest there is more cloud water associated with middle-level clouds on 17 November than DARLAM (dotted line). On 18 November, prior to the frontal passage, less cloud water is simulated with the SCMs. In ECHAM postfrontal clouds are simulated with a much higher cloud water path than in DARLAM. Observations of cloud cover (dotted–dashed line) indicate overcast skies for most of the second day. This is captured very well by ECHAM. In CCCma, the cloud cover and cloud water are both reduced to almost zero after the frontal passage. Cloud cover in the DARLAM simulation is considerably less than in the SCMs, again showing that the LAM simulation fails to produce the prefrontal middle-level cloud.

5. Discussion

The diagnosis of the model outputs from the satellite view produced model fields that could be directly compared with satellite retrievals in the ISCCP datasets. Some of the deficiencies in the model cloud simulations revealed by the model–satellite comparisons and the model–field observations were consistent. The satellite retrievals provided the tool to extend the spatial cov-

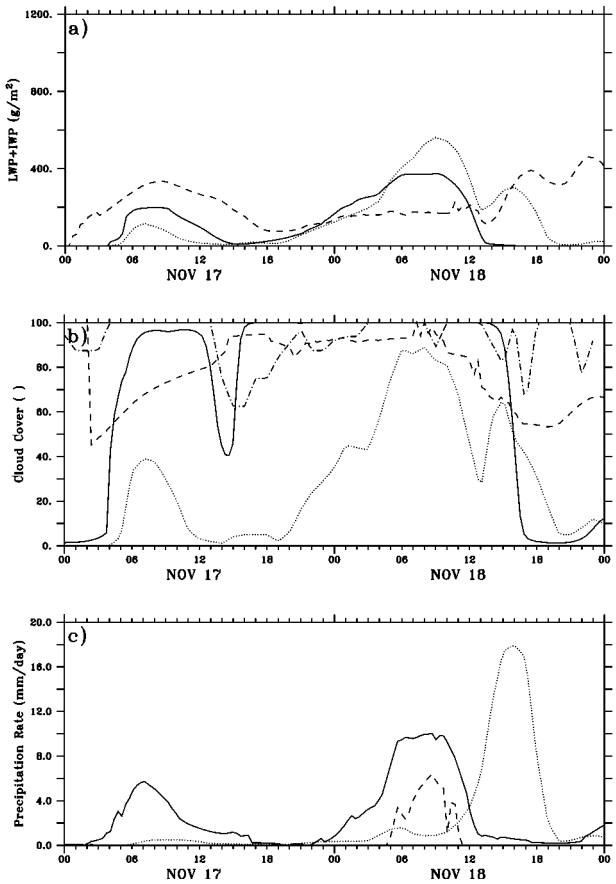

FIG. 12. (a) LWP + IWP, (b) total cloud cover, (c) and precipitation in the *Sprightly* column. DARLAM (BFR) is the dotted, ECHAM is the dashed, CCCma is the solid line, and the dotted–dashed line shows the observations.

erage of the comparisons and validate the model runs over the whole domain covered by the cloud system. For example, the low cloud deck behind the front in the early stages of its development, and the cirrus cloud deck at the storm's northern tail during its mature stage, were features that were outside the CFRP observational network. Model–satellite comparisons need to be further developed by producing model fields that are quantitatively equivalent to the satellite retrievals and they should be extended to include other satellite-retrieved fields such as rain amounts and cloud particle phase and sizes.

The MC2 CRM simulation showed that the CRMs developed much of the observed rainband structure. However, despite this increased horizontal resolution the generation of the middle-level cloud ahead of the front was still poor. The CRM simulations show that multiple cloud bands ahead of the front produced circulations not resolved by the LAMs. It is also likely that increased vertical resolution would generate an even better simulation and more realistic cloud fields.

The simulations using the LAMs were generally consistent. Generally they gave similar cloud amounts, although there were significant differences in the optical properties. The ISCCP–model comparisons showed that the correct generation of cloud fraction is not a sufficient condition to produce radiatively correct cloud fields in a GCM. Those comparisons showed that the accuracy of the prediction of cloud type is a function of the stage of development of the system. When the large-scale forcing was strong, such as along the front, the LAM simulations of both cloud cover and cloud type were very good. However, this was not the case when the forcing was weak.

All the LAM simulations developed mesoscale structures and captured the basic dynamic and thermodynamic structure of the front. However, all of the LAMs failed to capture some important facets of the cloud structure. In particular, while they all captured the upper-level cirrus cloud, they failed to develop any significant middle-level cloud ahead of the front. Both the ISCPP analyses and the surface observations support the conclusion that there is lack of middle-level cloud and an excess of cirrus cloud in the model simulations.

The LAMs and CRMs provide strong model evidence that the sublimation by the cirrus triggers the mesoscale descent. Below cloud base, cooling generates descending motions, which in the case of the upper-level cirrus acts to suppress the formation of middle-level clouds. These simulations demonstrate that diabatic processes represent both a physical reality and a model problem. The evaporation between 700 hPa and the surface is real and observations confirm that it is an important thermodynamic feature of the front. However, the sublimation of ice crystal from the cirrus well ahead of the front is too strong and may be responsible for suppressing the middle-level cloud. AGCMs operated in weather prediction mode are beginning to approach this resolution and they are likely to experience the same problem if the model misrepresents the cirrus physics.

The commonality of the physics packages is always an issue when intercomparing models. This case study would suggest that the different microphysical packages produced similar results. This assertion is based in the analysis of the two 300 km $\times$ 300 km regions centred over the M/V *Sprightly* and Mount Gambier. There was very little convective activity over the M/V *Sprightly* and all models gave similar large-scale rainfalls. However, significant activity over Mount Gambier and the ratio of convective rain to large-scale rain in the 20-km LAM simulations was strongly dependent on the moist convective schemes used in the model. The focus of this paper was not on the convective parameterization. However, model intercomparison also shows that even in a relatively simple case, such as the present case, the problems of interpretation will arise when different physics packages are used. The conclusions concerning the microphysical packages apply equally well to the SCMs. The major advantage of the SCM is that the impact of the microphysics can be studied in isolation from the feedback on the dynamics.

6. Conclusions

The primary aim of this paper was to develop a methodology to compare simulations of a frontal system from climate and low-resolution models with those of high-resolution cloud-resolving models. The study showed that, as expected, the higher-resolution models gave a more complete description of the front and captured more of the observed features of the front. The low-resolution simulations could not accurately capture the multiple-rainband structure because they lacked the nonlinear features present in the high-resolution simulations. In particular, it was demonstrated that when one of the LAMs was run with the coarse resolution typically used in climate models it failed to develop even the main frontal cloud band. The model intercomparision also identified problems in applying SCMs to rapidly advecting baroclinic systems. A new set of experiments using SCMs and CRMs needs to be designed before the worth of SCMs in frontal situations can be fully evaluated, or a new parameterization needs to be developed to account for the subgrid-scale gradients and variability. A key question not answered in the paper is the importance of vertical resolution in the overestimation of the high-level cloud and the underestimation of the middle-level cloud.

An important result coming from the study is that none of the models in the hierarchy can fully and accurately simulate the observed midlevel clouds. The key scientific questions arising from the midlevel cloud problem are the following:

- What is the feedback between frontal circulations and the cloud field?
- To what extent are the mesoscale circulations driven by subgrid-scale dynamical thermodynamical and microphysical processes?
- How can these subgrid-scale feedbacks be parameterized?
- Do the feedbacks lead to significant errors in NWP and climate models?
- To what extent do the subgrid-scale microphysical processes associated with frontal circulations contribute to the moistening of layers in the upper atmosphere?

The paper has provided the first step in a methodology to link individual case studies to climatological studies by showing that the same ISCCP techniques used to validate climatological studies can be applied to validate cloud properties in single case studies. The analysis of this typical Australian case has led to a number of critical advances toward realizing the overall goal of properly accounting for frontal systems within large-scale models. The techniques described in this paper have been applied to two other case studies with both weaker and stronger forcing over different storm tracks. A paper synthesizing the results from all three case studies will be published at a later date.

Acknowledgments. We would like to thank Bill Rossow for his ideas and suggestions, Alison Walker for her help with the case study ISCCP datasets, and ECMWF for providing reanalysis data.

This work contributes to the CSIRO Climate Change Research Program and is partly funded through Australia's National Greenhouse Program.

REFERENCES

Benoit, R., M. Desgagne, P. Pellerin, S. Pellerin, and Y. Chartier, 1997: The Canadian MC2: A semi-Lagrangian, semi-implicit wide band atmospheric model suited for finescale processes studies and simulation. *Mon. Wea. Rev.*, **125,** 2382–2415.

Browning, K. A., 1990: Organization of clouds and precipitation in extra-tropical cyclones. *Extratropical Cyclones: The Erik Palmén Memorial Volume*, C. Newton and E. O. Holopainen, Eds., Amer. Meteor. Soc., 129–153.

——, and Coauthors, 1993: The GEWEX Cloud System Study (GCSS). *Bull. Amer. Meteor. Soc.*, **74,** 387–399.

Chen, S. S., and W. M. Frank, 1993: A numerical study of the genesis of extratropical convective mesovorticies. Part I: Evolution and dynamics. *J. Atmos. Sci.,* **50,** 2401–2426.

Clough, S. A., and R. A. A. Frank, 1991: The evaporation of frontal and other stratiform precipitation. *Quart. J. Roy. Meteor. Soc.*, **117,** 1057–1080.

Eppel, D. P., H. Kapiza, M. Claussen, D. Jacob, W. Koch, L. Levkov, H. T. Mengelkamp and N. Werrmann, 1995: The non-hydrostatic mesoscale model GESIMA. Part II: Parameterizations and applications. *Beitr. Phys. Atmos.,* **68,** 15–41.

Flatau, P. J., G. J. Tripoli, J. Verlinde, and W. R. Cotton, 1989: The CSU RAMS cloud microphysics module: General theory and code documentation. Dept. of Atmospheric Science Paper 451, Colorado State University, 88 pp. [Available from Dept. of Atmospheric Science, Colorado State University, Fort Collins, CO 80523.]

Frank, W. L., and C. Cohen, 1985: Properties of tropical cloud ensembles estimated using a cloud model and an observed updraft population. *J. Atmos. Sci.*, **42,** 1911–1928.

——, and ——, 1987: Simulation of tropical convective systems. Part 1: A cumulus parameterization. *J. Atmos. Sci.,* **44,** 3787–3799.

Gibson, J. K., P. Kallberg, S. Uppala, A. Hernandez, A. Nomura, and Serrano, 1997: 1 ERA description. ECMWF Re-Analysis Project Rep. Series, 72 pp.

Gultepe, I., D. O'C. Starr, A. J. Heymsfield, T. Uttal, T. P. Ackerman, and D. L. Westphal, 1995: Dynamic characteristics of cirrus clouds from aircraft and radar observations in micro- and meso-γ scales. *J. Atmos. Sci.,* **52,** 4060–4078.

Kapitza, H., and D. P. Eppel, 1992: The non-hydrostatic mesoscale model GESIMA. Part I: Dynamic equations and tests. *Beitr. Phys. Atmos.,* **65,** 129–146.

Karstens, U., R. Nolte-Holube, and B. Rockel, 1996: Calculation of the water budget over the Baltic Sea catchment area using the regional forecast model REMO for June 1993. *Tellus,* **48A,** 684–692.

Katzfey, J. J., and B. F. Ryan, 1997: Modification of the thermodynamic structure of the lower troposphere by the evaporation of precipitation: A GEWEX cloud system study. *Mon. Wea. Rev.*, **125,** 1431–1446.

——, and ——, 2000: Midlatitude frontal clouds: GCM-scale modeling implications. *J. Climate,* **13,** 2729–2745.

King, W. D., 1982: Location and extent of supercooled regions in deep stratiform cloud in western Victoria. *Aust. Meteor. Mag.*, **30,** 81–88.

Kong, F., and M. K. Yau, 1997: An explicit approach to microphysics in MC2. *Atmos.–Ocean,* **35,** 257–291.

Kuo, H. L., 1974: Cumulus convection in weak and strong tropical disturbances. *J. Atmos. Sci.,* **31,** 1232–1240.

Lau, N.-C., and M. W. Crane, 1995: A satellite view of the synoptic-scale organization of cloud properties in midlatitude and tropical circulation systems. *Mon. Wea. Rev.,* **123,** 1984–2006

Levkov, L., B. Rockel, H. Kapitza, and E. Raschke, 1992: 3D mesoscale numerical studies of cirrus and stratus clouds by their time and space evolution. *Contrib. Atmos. Phys.,* **65,** 35–58.

Lohmann, U., and E. Roeckner, 1995: The influence of cirrus cloud-radiative forcing on climate and climate sensitivity in a general circulation model. *J. Geophys. Res.,* **100,** 16 305–16 323.

——, N. McFarlane, L. Levkov, K. Abdella, and F. Albers 1999: Comparing different cloud schemes of a single column model by using mesoscale forcing and a nudging technique. *J. Climate,* **12,** 438–461.

Majewski, D., 1991: The Europa-Model of the Deutscher Wetterdienst. *Proc. Seminar on Numerical Methods in Atmospheric Models,* Vol. 2, Reading, United Kingdom, ECMWF, 147–191.

McGregor, J. L., H. B. Gordon, I. G. Watterson, M. R. Dix, and L. D. Rotstayn, 1993: The CSIRO 9-level atmospheric general circulation model. CSIRO Division of Atmospheric Research, Tech. Paper 26, 89 pp. [Available from CSIRO Atmospheric Research, PMB1, Aspendale, VIC 3195, Australia.]

Moncrieff, M. W., and W. K. Tao, 1999: Cloud resolving models. *Global Energy and Water Cycles,* K. A. Browning and R. J. Gurney, Eds., Cambridge University Press, 200–212.

Randall, D. A., K.-M. Xu, R. J. Sommerville, and S. Iacobellis, 1996: Single-column models and cloud ensemble models as links between observations and climate models. *J. Climate,* **9,** 1683–1697.

Rossow, W. B., and R. A. Schiffer, 1991: ISCCP cloud data products. *Bull. Amer. Meteor. Soc.,* **72,** 2–20.

Rotstayn, L. D., 1997: A physically based scheme for treatment of stratiform clouds and precipitation in large-scale models. I: Description and evaluation of microphysical processes. *Quart. J. Roy. Meteor. Soc.,* **123,** 1227–1282.

Ryan, B. F., W. D. King, and S. C. Mossop, 1985a: The frontal transition zone and microphysical properties of associated clouds. *Quart. J. Roy. Meteor. Soc.,* **111,** 479–493.

——, K. J. Wilson, J. R. Garratt, and R. K. Smith, 1985b: Cold Fronts Research Programme: Progress, future plans, and research directions. *Bull. Amer. Meteor. Soc.,* **66,** 1116–1122.

——, ——, and E. J. Zipser, 1989: Modifications of the thermodynamic structure of the lower troposphere by the evaporation of precipitation ahead of a cold front. *Mon. Wea. Rev.,* **117,** 138–153.

Sundqvist, H., E. Berge, and J. E. Kristjansson, 1989: Condensation and cloud parameterization studies with a mesoscale numerical weather prediction model. *Mon. Wea. Rev.,* **117,** 1641–1657.

Tiedtke, M., 1989: A comprehensive mass flux scheme for cumulus parameterization in large-scale models. *Mon. Wea. Rev.,* **117,** 1779–1800.

——, 1993: Representation of clouds in large-scale models. *Mon. Wea. Rev.,* **121,** 3040–3061.

Tremback, C., G. Tripoli, R. Arritt, W. R. Cotton, and R. A. Pielkie, 1986: The Regional Atmospheric Modeling System. *Proceedings of an International Conference on Development Applications of Computer Techniques Environmental Studies,* P. Zannetti, Ed., Computational Mechanics Publication, Rewood Burn Ltd., 601–607.

Zang, G. J., and N. A. McFarlane, 1995: Sensitivity of climate simulations to the parameterization of cumulus convection in the Canadian Climate Centre General Circulation Model. *Atmos.–Ocean,* **33,** 406–446.